Journal of Ceramic Processing Research. Vol. 12, No. 1, pp. 102~105 (2011)

J O U R N A L O F
Ceramic Processing Research

The synthesis, thermal stability, crystal structure and spectroscopic study of $La_{0.80}Sr_{0.20}MnO_3$ powder obtained by the modified Pechini's method

Moisés R. Cesário[a,*], Daniel A. Macedo[b], Rosane M. P. B. Oliveira[b], Patrícia M. Pimentel[b], Roberto L. Moreira[c] and Dulce M. A. Melo[a,b]

[a]*Programa de Pós Graduação em Química – UFRN, CEP 59078-970, Natal/RN, Brazil*
[b]*Programa de Pós-Graduação em Ciência e Engenharia de Materiais – UFRN CEP 59072-970, Natal/RN, Brazil*
[c]*Departamento de Física – UFMG, CEP 30123-970, Belo Horizonte/MG, Brazil*

Strontium-doped lanthanum manganite ($La_{1-x}Sr_xMnO_3$) is a commonly used cathode in solid oxide fuel cells. In this study, $La_{0.80}Sr_{0.20}MnO_3$ powder was prepared by the modified Pechini's method using gelatin as the polymerizing agent. The polymeric resin obtained was characterized by thermogravimetric analysis and the powder calcined at 900 °C for 4 h has been characterized by X-ray diffraction, scanning electron microscopy and infrared spectroscopy. The $La_{0.80}Sr_{0.20}MnO_3$ phase exhibited rhombohedral symmetry. The infrared reflectance spectrum was dominated by a conduction mechanism besides the signature of less pronounced phonon features, characteristics of the crystal lattice. The present results indicated that the gelatin has been an efficient directional element to be used in $La_{0.80}Sr_{0.20}MnO_3$ synthesis, and it is a low cost material, non toxic and makes the polymeric precursor synthesis less complicated.

Key words: Strontium-doped lanthanum manganite, modified Pechini's method, gelatin.

Introduction

Strontium-doped lanthanum manganite ($La_{1-x}Sr_xMnO_3$ or LSM) has been extensively investigated and developed as a high temperature solid oxide fuel cell cathode due to its high catalytic activity for oxygen reduction, high electrical conductivity and a thermal expansion coefficient similar to that of the yttria stabilized zirconia (YSZ) electrolyte. Strontium is the preferential element chosen as a dopant of the cathodic material of the SOFCs to allow the attainment of higher electronic conductivity, which is because of the increase of Mn^{4+} ions formation and for the substitution of La^{3+} for Sr^{2+} ions [1-3].

Several techniques are available for the preparation of LSM powders, e.g. Pechini's method, a solid state reaction, spray pyrolysis, sol-gel, coprecipitation, combustion process etc. [4-10]. Each method has its own characteristics. Pechini's method or the polymeric precursor method is based on metallic citrate polymerization using ethylene glycol. A hydrocarboxylic acid, such as citric acid, is used to chelate cations in an aqueous solution. The addition of a glycol such as ethylene glycol leads to the formation of an ester. The polymerization reaction, promoted by heating the mixture, results in a homogeneous resin in which metal ions are uniformly distributed throughout the organic matrix. A primary thermal treatment in an oxidizing atmosphere around 250-350 °C produces the so-called precursor powder. This method presents advantages such as good homogeneity, good stoichiometric control and good control of the particle morphology [11, 12]. Usually the powders obtained by Pechini's method contain a large amount of organic material that must be eliminated at high temperatures to synthesize pure oxides.

An alternative method for preparing nanoparticles of metal oxides such as Cr_2O_3 and NiO with a particle size of the order of nanometres has been developed using commercial gelatin as an organic precursor. Gelatins have also been used to obtain silica and metallic AuNi nanoparticles with low annealing temperatures, and this method has been named by the authors as a *soft chemical route* [13, 14].

In this study, we report the preparation of strontium-doped lanthanum manganite with a nominal composition $La_{0.80}Sr_{0.20}MnO_3$ (LSM 20) by the modified Pechini's method using gelatin as polymerizing agent and its characterization by TG, XRD, SEM, FAR and MID-Infrared spectroscopies.

Experimental

The starting materials used to prepare $La_{0.80}Sr_{0.20}MnO_3$ (LSM 20) powder were: lanthanum nitrate ($La(NO_3)_3{\cdot}6H_2O$, > 99.0% VETEC, Brazil), strontium nitrate ($Sr(NO_3)_2$, > 99.0% VETEC, Brazil), manganese nitrate ($Mn(NO_3)_2{\cdot}4H_2O$, > 97.0% VETEC, Brazil), citric acid (> 99.0% VETEC, Brazil), deionized water and commercial gelatin. The synthesis procedure is described in Fig. 1, in which

*Corresponding author:
Tel : +55-84-99831115
Fax: +55-84-32153825
E-mail: romolosquimica@hotmail.com

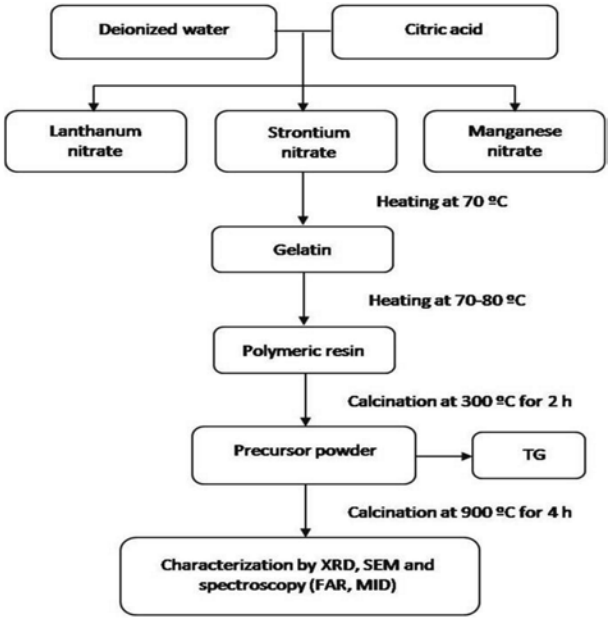

Fig. 1. Flowchart for the synthesis of LSM 20 powder by the modified Pechini's method.

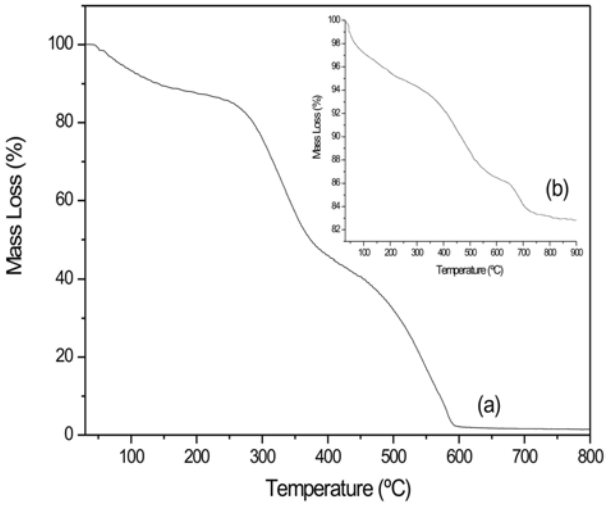

Fig. 2. TGA curves for (a) gelatin and (b) precursor powder of the LSM 20.

the molar ratio of metal/citric acid was fixed at 1 : 2. The gelatin was added in a weight ratio of 2 : 3 (citric acid/gelatin) and the solution was thoroughly stirred by a magnetic mixer until a polymeric resin was formed which was calcined at 300 ºC for 2 h at a heating rate of 10 K·minute^{-1} to produce the precursor powder of the $La_{0.80}Sr_{0.20}MnO_3$ phase.

A Shimadzu differential thermal analyzer was used to make thermogravimetric (TGA) measurements in air flow (flow rate of 50 ml minute^{-1}) in the temperature range from 25 to 900 ºC with a heating rate of 10 K·minute^{-1}. The precursor powder was calcined at 900 ºC for 4 h and its structural characterization was performed by X-ray diffraction using a Shimadzu XRD-7000 diffractometer, with a 2θ angle scan between 20º and 80º, with 0.02º scans and counting time of 0.6 s per scan, using monochromatic copper-Kα radiation (λ = 1.5418 Å) obtained with 40 kV and 30 mA filament current. Rietveld refinement of the X-ray diffraction pattern was made using BDWS-9807 Software. The pseudo-Voigt function was chosen to fit the peak profiles for all identified crystalline phases. The morphological analysis of the particles was performed by field emission scanning electron microscopy. An infrared reflectance spectrum of a sample pellet was recorded with a Fourier-transform spectrometer (Bomem DA 8-02) equipped with a fixed-angle specular reflectance accessory (external incidence angle of 11.5º). For these measurements, the sample was prepared in the form of a disk of 13 mm diameter and pressed (150 MPa) in a vacuum with a relatively smooth surface. A gold mirror was used as reference. In the MID-infrared region (500 to 4000 cm^{-1}), a SiC glow-bar lamp was used as an infrared source, a Ge-coated KBr beamsplitter, and a liquid nitrogen cooled HgCdTe detector. In the far-infrared range (50-600 cm^{-1}), a mercury-arc lamp was employed, a 6 μm coated Mylar hypersplitter, and a liquid helium cooled Si-bolometer. The measurements were performed at a pressure of 10^{-4} bar and with a spectral resolution of 2 cm^{-1}.

Results and Discussion

The thermogravimetric analysis (TGA) curves obtained for the gelatin and LSM 20 calcined at 900 ºC are shown in Fig. 2. It can be seen that the decomposition of gelatin, that consists of glycine (Gly) and proline (Pro), presents three distinct steps. First, there is a small mass loss between room temperature and around 100 ºC associated with humidity. In the second step the reduction of mass can be attributed to the elimination of fragments of amino acids, usually Pro, which is thermodynamically susceptible to thermal degradation in an oxidizing atmosphere. The last step of thermo decomposition would be associated to the oxidation of the all the contents of Gly, which are completely degraded between 500 ºC and 590 ºC, this step also presents a reduction of the mass of amino acid, which are bonded to minerals present in the gelatin.

For the LSM 20 powder, the thermal decomposition process occurs in five steps between 30 and 900 ºC and the total mass loss is 17.19%. The first step of thermal decomposition (between 30 and 190 ºC) is related to the loss of water and gases adsorbed on the surface of the powder. Polymer degradation occurs in the second and third steps. This process is characterized by an abrupt fall in the mass loss at around 525 ºC. In the fourth step (between 650 and 750 ºC) the mass loss is attributed to carboxylate decomposition and the formation of a carbonaceous phase. Finally, the material begins to stabilize at 750 ºC (fifth step) when the oxide phase formation has been confirmed from the XRD study.

Fig. 3 displays the XRD pattern of the powder calcined at 900 ºC for 4 h. XRD result indicates the formation of

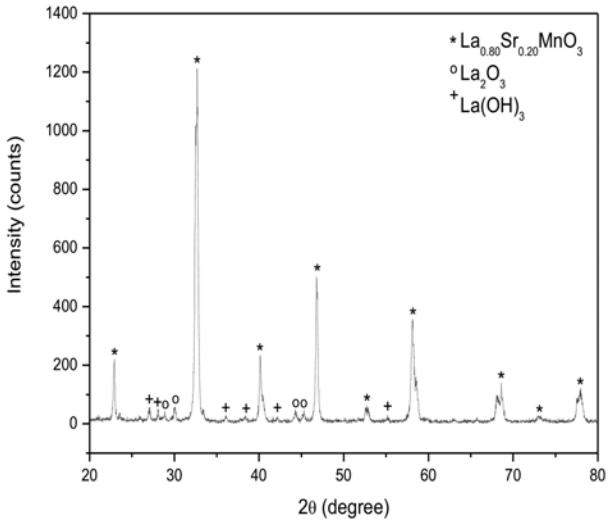

Fig. 3. XRD pattern of the LSM 20 powder calcined at 900 ºC for 4 h.

the LSM perovskite structure, according to JCPDS file 53-0058. The powder also exhibited extra peaks corresponding to La_2O_3 and $La(OH)_3$ phases. The formation of the La_2O_3 phase might be due to the decomposition of $(LaO)_2CO_3$, proceeding from the incomplete complexation of the La^{3+} ions. Gaudon *et al*. also reported the presence of La_2O_3 in strontium-doped lanthanum manganite [15]. The hydration of the La_2O_3 at high temperatures leads to the appearance of the $La(OH)_3$ compound. Yang *et al*. [16] observed many other phases (SrO, La_2O_3 and Mn_3O_4) in LSM synthesized by Pechini's method and calcined at 900 ºC.

The crystal structure of the powder has been evaluated by a Rietveld refinement using BDWS-9807 Software (Fig. 4). The quantitative phase analysis, lattice parameters (*a, b and c)*, crystallite size, microstrain, and refinament indexes are given in Table 1.

The refinement quality can be checked by the S value,

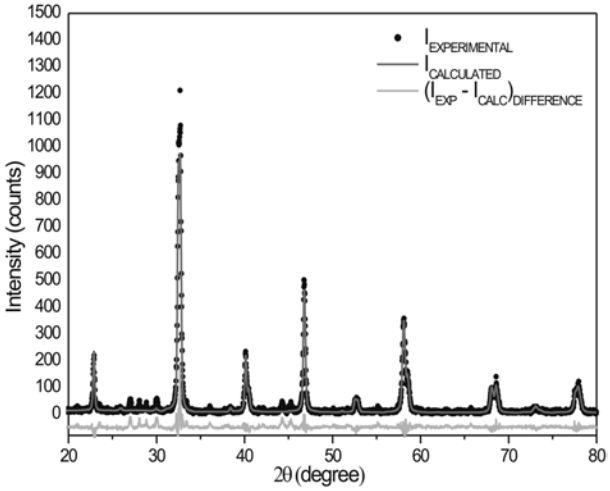

Fig. 4. Rietveld refinement performed for the LSM 20 powder.

Table. 1. Quantitative phase analysis, lattice parameters, crystallite size, microstrain, and refinement indexes of the LSM 20 powder evaluated by a Rietveld refinement

Structure: rhombohedral		Space group: $R\bar{3}c$		
Mol% phase $La_{0.80}Sr_{0.20}MnO_3$	Lattice parameters (Å)	Crystallite size (nm)	Microstrain (%)	Refinement indexes
96.23	$a = 5.4972$	36.49	0.0797	$R_{wp} = 26.07$
	$b = 5.4972$			$R_{exp} = 18.20$
	$c = 13.3553$			$S = 1.43$

which is obtained by the expression S = Rwp/Rexp. The low S value obtained in this study indicates that the data were successfully refined. The $La_{0.80}Sr_{0.20}MnO_3$ phase exhibited rhombohedral symmetry with space group $R\bar{3}c$, in concordance with the literature [10, 17]. The secondary phases La_2O_3 and $La(OH)_3$ were quantified as 0.23 mol% and 3.54 mol%, respectively. For the $La_{0.80}Sr_{0.20}MnO_3$ phase the value obtained for the crystallite size was comparable to those reported in the literature for LSM 15 and LSM 22 powders obtained by Pechini's method calcined at 900 ºC [6].

The morphological analysis of the particles by scanning electron microscopy (FE-SEM) is displayed in Fig. 5. The

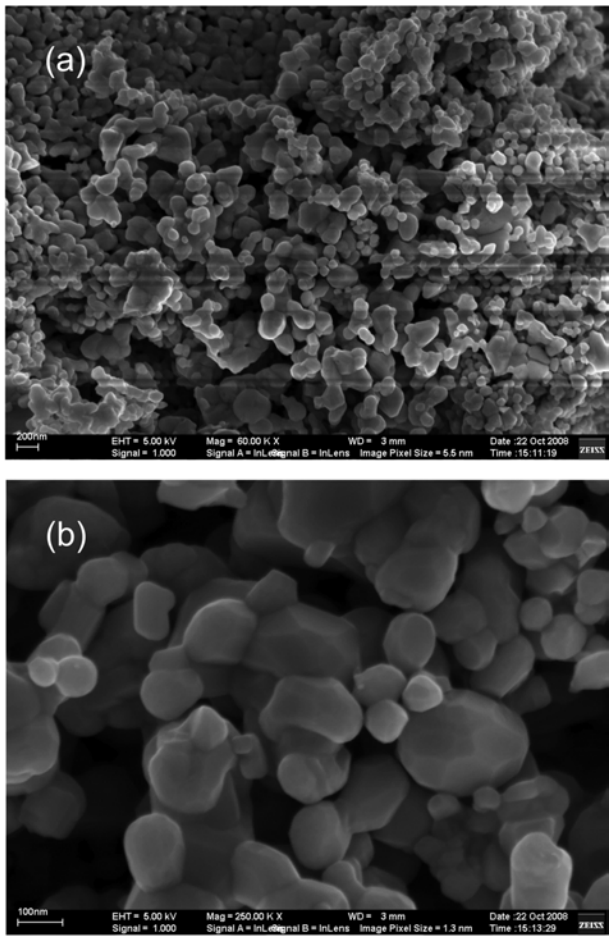

Fig. 5. SEM micrographs for the LSM 20 powder calcined at 900 ºC for 4 h: a) scale bar: 200 nm and b) scale bar: 100 nm.

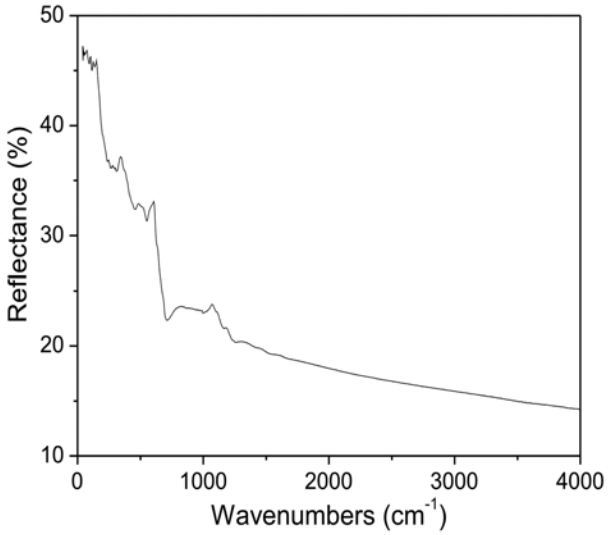

Fig. 6. Infrared reflectance spectrum for the LSM 20 powder, in the FAR and MID ranges.

powder exhibits particles in an almost-spherical morphology with the presence of nanoparticle agglomerates. The coalescence of the particles shows a heterogeneous particle size range from 50 to 300 nm. The difference between the particle size and crystallite size (< 40 nm) indicates the presence of agglomerates, since when the particle size is roughly equal to the crystallite size, we have a monodispersed powder, that is, an agglomerate-free powder [18].

The infrared reflectance spectrum in the FAR and MID infrared ranges altogether, is presented in Fig. 6. The almost continuous decrease of reflectivity with wavenumber shows that this spectrum is dominated by a conduction mechanism [19]. Moreover, first order phonon features characteristic of the crystal lattice are well seen superposed on the decreasing reflectivity curve below 700 cm^{-1}. The reflectivity lineshape of these phonons is rather characteristic of conducting materials and denotes possibly electron-phonon coupling in LSM 20, as also observed in $La_{0.7}Ca_{0.3}MnO_3$ ceramics [20]. On the other hand, the two modes above 1000 cm^{-1} are likely to be defect modes from impurities due to unreacted materials, as observed by XRD.

Conclusions

LSM 20 powder with a rhombohedral structure and small amounts of secondary phases La_2O_3 and $La(OH)_3$ have been synthesized by the modified Pechini's method using gelatin as the polymerizing agent. The total mass loss in the precursor powder was 17.19% and this occurred in five steps between 30 and 900 ºC. The thermogravimetric analysis also indicated that the formation of the oxide phase begins at 750 ºC. The powder calcined at 900 ºC for 4 h exhibited particles with an almost-spherical morphology with the presence of nanoparticle agglomerates. The $La_{0.80}Sr_{0.20}MnO_3$ phase crystallized in the $R\bar{3}c$ space group and exhibited characteristic phonon modes besides charge carrier contributions to the optical conductivity. The phonon line shapes suggest strong electron-phonon coupling. These results indicate that LSM powder has been suitably synthesized using gelatin as the polymerizing agent. The gelatin is a low cost material, non toxic and makes the polymeric precursor synthesis less complicated. The powder obtained can be used as a cathode material for high temperature solid oxide fuel cells.

Acknowledgements

This work has been partially supported by the Brazilian agencies CAPES (Coordenação de Aperfeiçoamento de Pessoal de Nível Superior) and Fapemig (Fundação de Amparo à Pesquisa de Minas Gerais).

References

1. N.Q. Minh, J. Am. Ceram. Soc. 76 (1993) 563-588.
2. T. Ruifen, F. Jue, L. Yali and X. Changrong, J. Power Source 185 (2008) 1247-1251.
3. A. Ghosh, A.K. Sahu, A.K. Gulnar and A.K. Suri, Scr. Mater. 52 (2005) 1305-1309.
4. M.P. Pechini, US Patent #3.330.697, July 11, 1967.
5. L. Conceição, C.R.B. Silva, N.F.P. Ribeiro and M.M.V.M. Souza, Mater. Charact. 60 (2009) 1417-1423.
6. B. Cela, D.A. Macedo, G.L. Souza, R.M. Nascimento, A.E. Martinelli and C.A. Paskocimas, J. New Mat. Electrochem. Systems 12 (2009) 109-113.
7. D. Grossin and J.G. Noudem, Solid State Sci. 6 (2004) 939-944.
8. R.S. Guo, Q.T. Wei, H.L. Li and F.H. Wang, Mater. Lett. 60 (2006) 261-265.
9. D. Berger, C. Matei, F. Papa, D. Macovei, V. Fruth and J.P. Deloume, J. Eur. Ceram. Soc. 27 (2007) 4395-4398.
10. B.M. Nagabhushana, C.R.P. Sreekanth, K.P. Ramesh, C. Shivakumara and G.T. Chandrappa, Mater. Res. Bull. 41 (2006) 1735-1746.
11. K.P. Lopes, L.S. Cavalcante, A.Z. Simões, J.A. Varela, E. Longo and E.R. Leite, J. Alloys Compd. 468 (2009) 327-332.
12. R.A. Candeia, M.I.B. Bernardi, E. Longo, I.M.G. Santos and A.G. Souza, Mater. Lett. 58 (2004) 569-572.
13. A.M.L. Medeiros, M.A.R. Miranda, A.S. Menezes, P.M. Jardim, L.R.D. Silva, S.T. Gouveia and J.M. Sasaki, J. Metastable Nanocrystalline Mater. 20 (2004) 399-406.
14. A.O.G. Maia, C.T. Meneses, A.S. Menezes, W.H. Flores, D.M.A. Melo and J.M. Sasaki, J. Non-Cryst. Solids 352 (2006) 3729-3733.
15. M. Gaudon, C.L. Robert, F. Ansart, P. Stevens and A. Rousset, Solid State Sci. 4 (2002) 125-133.
16. W.D. Yang, Y.H. Chang and S.H. Huang, J. Eur. Ceram. Soc. 25 (2005) 3611-3618.
17. E. Konysheva, J.T.S. Irvine and A. Besmehn, Solid State Ionics 180 (2009) 778-783.
18. R.C. Pessoa, M.C. Nasar, R.S. Nasar and I.V.P. Yoshida, Cerâmica 54 (2008) 253-258.
19. A.M.H. Gosnet, M. Koubaa, A.F. Santander-Syro, R.P.S.M. Lobo, P. Lecoeur and B. Mercey, Phys. Rev. B 78 (2008) 115-118.
20. K.H. Kim, J.Y. Gu, H.S. Choi, J.W. Park and T.W. Noh, Phys. Rev. Lett. 77 (1996) 1877-1880.